THE CONNECTION RESPONSE OF ROCKING TIMBER WALLS

M. P. Newcombe

General Manager, Kirk Roberts Consulting Engineers, Auckland, New Zealand. Email: michaeln@kirkroberts.co.nz

ABSTRACT

Structural systems that incorporate rocking timber walls are becoming more prevalent in New Zealand. This is due primarily to the application of new post-tensioned timber systems in several buildings and the increased use of solid timber construction in the form of Cross-Laminated Timber (CLT), Laminated Veneer Lumber, Glue-laminated timber (Glulam) and round wood throughout New Zealand.

In the past, simplistic design approaches have been applied to determine the lateral strength of rocking timber walls, which do not assess the compression stresses in the timber. However, new rocking wall systems can introduce high axial loads (due to the application of post-tensioning or multi-storey gravity loads) that result in high compression stresses within rocking connections. Furthermore, for post-tensioned timber walls the tension in tendons (and hence the lateral strength of the wall) depends on the rotation and the length of the compression region within the connection. Therefore, more advanced analysis methods are required to evaluate strength and material strains for these systems.

This paper introduces a new approach for assessing the connection response of rocking timber walls. Using this approach, the depth of the compression region, the compression stresses in the timber and the moment capacity of a rocking wall connection can be more accurately determined. The design approach is calibrated using a finite element (FE) sensitivity study and is validated using experimental data.

1 INTRODUCTION

Rocking timber walls can be characterised as a timber panel which allows uplift at the base of the wall when subject to lateral loads (see Figure 1). Timber rocking walls have been used for decades in the form of Cross-Laminated Timber (CLT) or Triboard Panels, and plywood or strand board shear walls (where the strength of the wall is governed by the hold-downs). Generally axial loads on these wall panels are small and result in a small compression zone (or neutral axis depth) at the base of the wall when subjected to lateral loads. This allows the moment capacity of a wall-base connection to be assessed relatively accurately by assuming that the centre of compression is at the edge of the wall and taking moments from the edge of the wall to the hold-down connections [1].

However, recent advances in timber engineering have led to post-tensioned (PT) timber walls [2], based on similar systems in pre-cast concrete [3-5], and medium-rise multi-storey timber buildings.

Post-tensioning introduces high axial loads into the wall panels, affecting the neutral axis depth and consequently the connection moment capacity. Also, the post-tensioning force applied to the wall depends

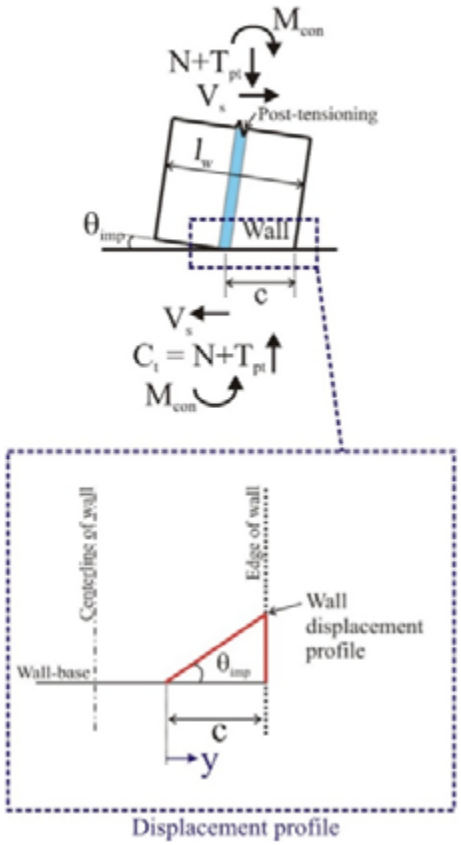

Figure 1: *Rocking post-tensioned timber wall equilibrium condition and connection deformation*

on gap opening at the rocking interface which is a function of the connection rotation and the neutral axis depth. Therefore, simple design methods (discussed above) may be inaccurate and provide no indication of the compression stresses in the timber at the connection.

Procedures have been proposed to determine the moment-rotation response (including neutral axis depth and compressive stresses) of rocking connections for PT precast concrete walls [6-8]. Because strain compatibility (or Bernoulli) assumptions do not apply at the connection interface (after decompression), these procedures rely on the Monolithic Beam Analogy (MBA) [6, 7] to determine strains and stresses within the neutral axis, as a function of the imposed rotation, θ_{imp}, and neutral axis depth of the connection. The MBA was applied to PT timber walls by Newcombe et al [9], where the following expression was proposed:

$$\varepsilon_c = \left(\frac{3\theta_{imp}}{L_{cant}} + \phi_{dec}\right)c \qquad [1]$$

Where: ε_c = the timber compressive strain at the extreme fiber;

$L_{cant} = H_e$ = the shear span or effective height of the wall;

$\phi_{dec} = \frac{2\sum N_{dec}}{E_{para} t_w l_w^2}$ is the decompression curvature;

$\sum N_{dec}$ is the sum of the axial forces applied to the wall at decompression;

E_{para} is the parallel to grain elastic modulus;

I_w is the second moment of inertia of the wall element;

l_w is the length of the wall element.

To determine the elastic stress in the timber at the extreme compression fiber, f_c, an effective connection modulus, E_{con}, was proposed. It is suggested by Newcombe [10] and Marriott [11], that the effective connection modulus is not equal to the parallel-to-grain elastic modulus. It was proposed [10] that due to end effects of parallel-to-grain timber in compression, a reduced elastic modulus is required when modelling the connection response termed E_{con}. Therefore:

$$f_c = E_{con}\varepsilon_c \qquad [2]$$

Where: $E_{con} = 0.55E_{para}$.

These expressions are used in the EXPAN Post-Tensioned Timber Buildings – Design Guide [12], where the reduction in the elastic modulus at the connection is termed k_{gap}.

However, Newcombe 2012 [13] raised questions regarding the accuracy of the MBA approximation when applied to post-tensioned timber walls. Key points are:

- Due to the relatively low compressive stiffness of timber (compared to concrete and steel), the neutral axis depth for PT timber connections is highly variable within the range of expected connection rotations. Hence, the key assumption made by the MBA for concrete and steel (that the compressive strain in material can be represented by an equivalent monolithic member) may not be sufficiently accurate.
- Intuitively it is unreasonable to assume that the strain in the timber at the connection interface is related to the shear span, L_{cant}, and hence the height of the wall, as shown in Equation 1. As the height of the wall increases the connection response should not be significantly affected.
- The calibrated effective connection modulus, E_{con}, and the shear span, L_{cant}, may result in a significant underestimation of the strain in the timber. Hence, for a given design level, there may be significantly more damage to the wall elements than expected.

Therefore, this paper presents a new methodology to relate the neutral axis depth, the strain in the timber and connection rotation for rocking timber walls (based on work by Newcombe 2012 [13]). This approach is calibrated using Finite Element modelling and validated using experimental results from previously published works.

2 WSA DESIGN APPROACH

The proposed design approach is a Winkler-Spring Analogy (WSA) with a constrained displacement profile within the neutral axis depth. This enables the formulation of a relationship between the neutral axis depth and the imposed connection rotation (termed the θ_{imp}-c relationship) within the elastic range of the timber. This formulation is only appropriate beyond the decompression point of the connection. Prior to the decompression point, normal Bernoulli assumptions are appropriate.

Based on experimental evidence [10], the compressive deformation of the wall inside the neutral axis depth (after the decompression point) is linear (see Figure 1).

If it is assumed that the wall foundation is effectively rigid the displacement profile can be written as:

$$\delta(y) = \theta_{imp} \cdot y \quad y = 0 \rightarrow c \qquad [3]$$

Where: y is the distance from the neutral axis depth within the neutral axis.

If it is assumed that the axial stiffness of the timber is constant with y, then the stress in the timber, f_t, can be defined as:

$$f_t(y) = \left(\frac{\theta_{imp}}{L_e} + \phi_{dec} \right) E_{para} \cdot y \quad y = 0 \rightarrow c \qquad [4]$$

Where: L_e is the effective length of an equivalent Winkler spring

The compression applied by the timber, C_t, must be in equilibrium with the sum of any axial forces applied to the wall, ΣN. Hence:

$$C_t = \sum N = t_w \int_0^c f_t(y) dy \ldots$$

$$= \left(\frac{\theta_{imp}}{L_e} + \phi_{dec} \right) \frac{E_{para} t_w c^2}{2} \qquad [5]$$

Where: t_w is the thickness of the wall

Rearranging the above expression in terms of the neutral axis depth gives:

$$c = \left(\frac{2 \sum N}{\left(\frac{\theta_{imp}}{L_e} + \phi_{dec} \right) E_{para} t_w} \right)^{0.5} \qquad [6]$$

For PT walls the force applied by the post-tensioning depends on the neutral axis depth and connection rotation. Therefore, iteration of the above force-equilibrium equation will be required to determine the neutral axis depth.

3 CALIBRATION OF WSA

There is no obvious physical parameter that defines the effective spring length for walls and enables the computation of the neutral axis depth (using Equation 6). Therefore, finite element (FE) sensitivity study is used to calibrate the effective length.

3.1 FE MODELS

The FE models are created in SAP 2000 [14] using a fine mesh of shell elements, as shown in Figure 2. Firstly, a benchmark wall model was created. Then individual properties of the benchmark model were modified forming a sensitivity study of 44 FE models. Properties that were altered were wall geometry, post-tensioning force, lateral load, wall height and material properties (refer to Newcombe [13] for further detail). The sensitivity study ensures a robust evaluation of the accuracy of the analytical (θ_{imp}-c) relationship.

The boundary conditions consist of a pin supports at the base of the wall, which resist only longitudinal compression and shear forces. Hence, restraint were removed if tension forces occur, which is an iterative process. Notably, it is assumed that all shear transfer at the rocking connection interface is within the compression region and not via shear keys or connections at other locations.

A lateral load is applied to the top of the wall that generates a known connection moment. This lateral load is distributed evenly throughout the top of the wall section to avoid unrealistic stress concentrations. Axial loads (730kN for the benchmark model) are applied to the top of the wall to simulate the compression provided by post-tensioning and/or gravity loads, which are kept constant throughout the analysis. Orthotropic material properties based on Laminated Veneer Lumber (LVL) are used for the FE shell elements as shown in Table 1 and are based on research by Murray [15].

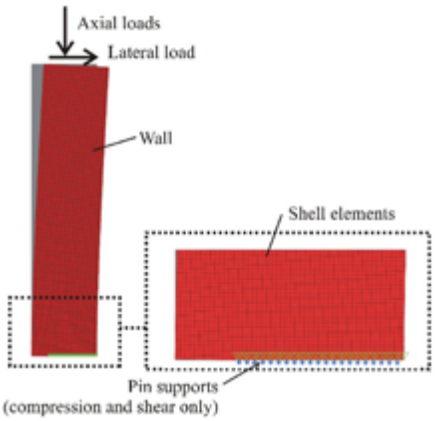

Figure 2: *Boundary conditions and applied loads for the benchmark FEM of the wall*

Table 1: Material properties for the benchmark wall model

Parameter	Symbol	Units	Value
Elastic modulus – Parallel to grain	E_{para}	MPa	13200
Elastic modulus – Perp. to grain	E_{perp}	MPa	660
Poisson's ratio	υ	-	0.3
Shear modulus	G	MPa	600

3.2 INTERPRETATION OF FE MODELS

To evaluate the accuracy of the proposed θ_{imp}-c relationship, the results from each FE model must be interpreted accurately. The neutral axis depth can be readily identified by observing the longitudinal stresses, but the imposed connection rotation is more difficult to determine. This is because the deformation at the base of the wall outside the neutral axis depth does not remain linear (see Figure 5) and is effected by axial and shear stresses at the connection interface.

Therefore, the connection rotation is deduced by taking the total deformation of the wall, Δ_{tot}, and subtracted the elastic deformation of the wall element. Hence:

$$\theta_{imp} = \frac{\Delta_{tot}}{H} - \left(\theta_f + \theta_s\right) \qquad [7]$$

The flexural and shear deformation of the wall is approximated using simple beam theory.

Therefore:

$$\theta_f = \frac{\Delta_f}{H} = \frac{FH^2}{3E_{para}I_w} \qquad [8]$$

And:

$$\theta_s = \frac{\Delta_s}{H} = \frac{F}{GA_{sw}} \qquad [9]$$

Where: F is the lateral load;
I_w is the second moment of inertial;
H is the height of the wall;
$A_{sw} = \frac{2}{3} l_w t_w$ is the shear area

The shear area used in simple beam theory is only an approximation, which can affect the accuracy of the computed imposed rotation. If shear deformation is ignored in the model, the imposed rotation at the connection can be determined more accurately. However, if the shear modulus significantly affects neutral axis depth, the accuracy of the proposed θ_{imp}-c relationship may be affected. This was investigated as part of the sensitivity study by creating models with and without shear deformation.

3.3 CALIBRATION OF THE EFFECTIVE LENGTH

The following steps were followed to calibrate the effective length (of the equivalent Winkler Springs) for the WSA approach:

1. The effective length is guessed.
2. The neutral axis depth is computed using Equation 6, considering the imposed rotation inferred from the FE models (see Equation 7).
3. The computed neutral axis depth (c_{eqn}) is compared with the neutral axis depth from the FE models (c_{FEM}).
4. The effective length is adjusted and steps 2 to 4 are repeated until the c_{eqn} equals c_{FEM}.

Once effective lengths have been calibrated for each of the 44 FE models, an empirical equation for the effective length is proposed. The effective lengths given by this equation approximately match the calibrated values and take into account influential design parameters.

3.4 RESULTS

The effective spring length is not constant and varies with the wall length, the neutral axis depth, and to a lesser extent the orthotropic properties of the timber. The parameter that caused the most significant variation in the effective length was the ratio of the wall length and neutral axis depth (l_w/c). As shown in Figure 3, as the l_w/c ratio increases the stresses at the toe of the wall become more disturbed (and less Bernoulli), which tends to reduce the axial stiffness and increase the effective length. In Figure 3, red corresponds to the peak compressive stress and blue is zero stress.

Based on the results of the FE models an empirical relationship is proposed to define the effective length for walls:

$$L_e = 120\left(\frac{l_w}{c} - 1\right) \quad (mm) \qquad [7]$$

Because both the effective length and the imposed rotation depend on the neutral axis depth, iteration is required. The predicted neutral axis depth from Equations 6 and 7 is compared with the results from the FE models in Figure 4.

The neutral axis depth obtained from Equations 6 and 7 is in good agreement with the FE results. It was determined that the inclusion or exclusion of the longitudinal shear modulus (G_{12}) did not significantly affect the calibrated effective length (see Figure 4).

The deformation profile at the base of the wall outside the neutral axis depth was found to be significantly non-linear (see Figure 5a). The procedure described in section 3.2 gives an approximate imposed rotation about the centre of gravity of the section (see the linear approximation in Figure 5a). Therefore, reinforcement connected towards the tension edge of the wall may be subjected to larger displacements than predicted.

Furthermore, the non-linearity at the base of the wall has implications for experimental testing. Potentiometers are used at the base of the rocking timber walls to define the neutral axis depth (see Figure 5b) assuming the deformation profile outside the neutral axis depth is linear. If this is not the case, then the experimentally-inferred neutral axis depths may be inaccurate.

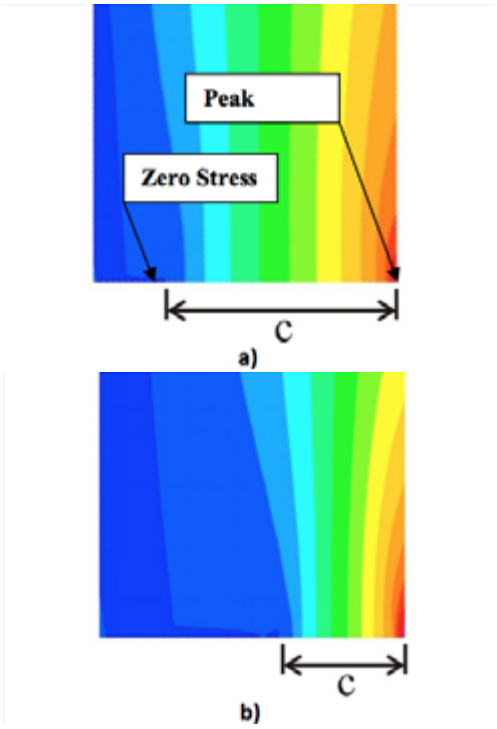

Figure 3: *Longitudinal stresses at the base of the wall: a) $c/l_w = 0.75$ b) $c/l_w = 0.41$*

4 VALIDATION OF WSA

The accuracy of the WSA procedure was validated by comparing experimental data from Iqbal et al [16] and Smith et al [17] for two thirds-scale wall subassembly tests.

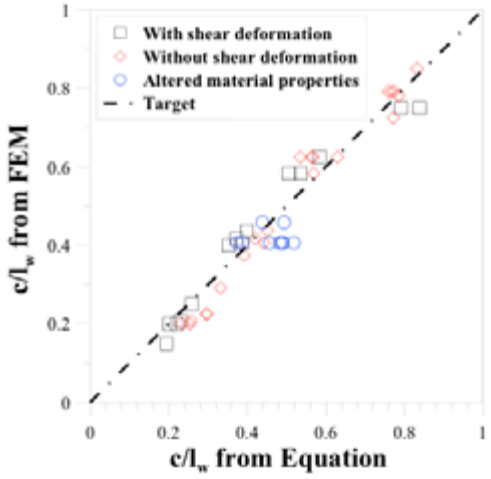

Figure 4: *Correlation between the predicted and FEM neutral axis depth*

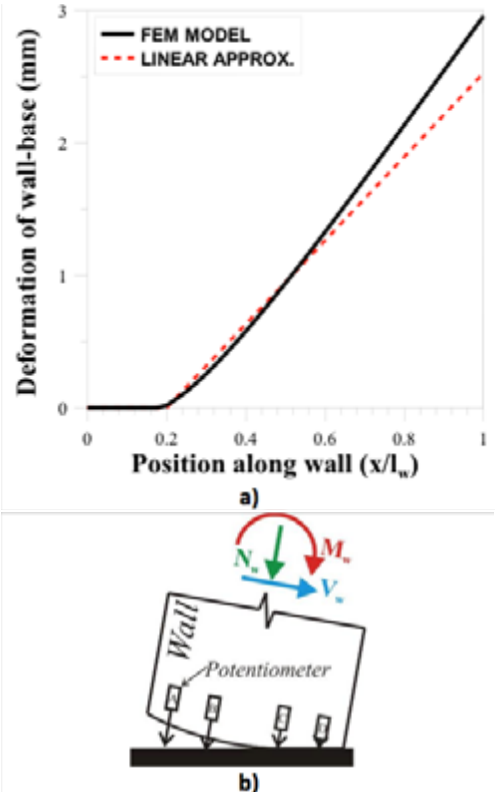

Figure 5: *Displacement profile at the base of the walls a) Example FEM model c b) Diagram with potentiometers*

As shown in Figure 6, the analytical predictions match well with experimental data (refer to Newcombe [13] for more information).

Notably, if the same wall is modelled using the Monolithic Beam Analogy (as applied by Newcombe et

al [9]) the predicted peak strain in the timber for a given connection rotation is an order of magnitude lower than that predicted by the WSA approach. Yet, due to the high parallel-to-grain compressive strength of laminated veneer lumber and low post-tensioning forces, the timber at the base of the wall remains within the elastic range for both methods. This may not be the case when higher levels of post-tensioning are applied.

Further validation of the WSA procedure is necessary. Due to inaccuracies in determining the neutral axis depth during experimental testing (discussed above) limited data is available for comparison with the WSA model. As shown in Figure 6c, experimental data can fail to yield a meaningful neutral axis depth relationship. However, visual inspection (Figure 6c) indicates that the neutral axis depth predicted by the WSA approach is relatively accurate. Also, this study is limited to the elastic response of the timber. Hence, the appropriateness of the WSA model should be assessed for inelastic response of the timber.

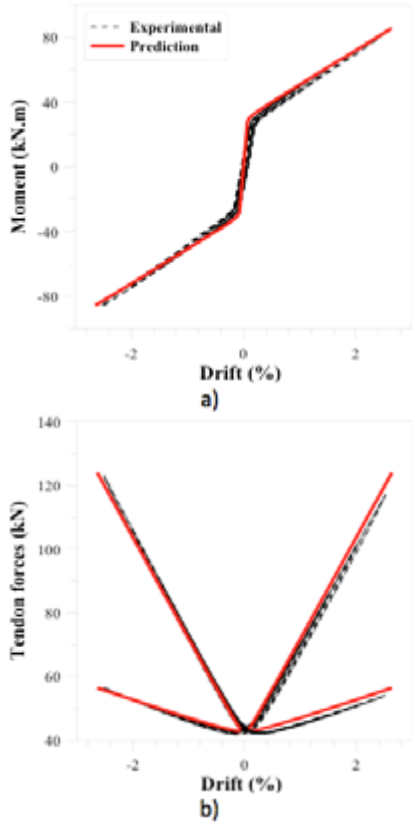

Figure 6: *Experimental - analytical comparison for Subassembly: a) Connection moment b) Tendon forces c) Neutral axis depth d) Observed neutral axis depth at 2.5% drift*

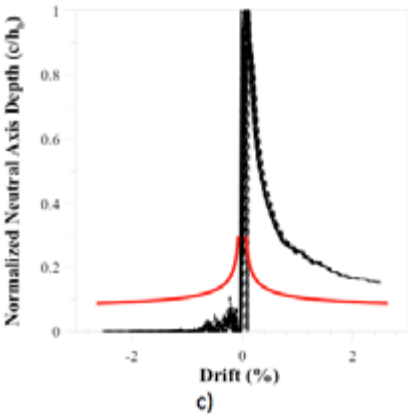

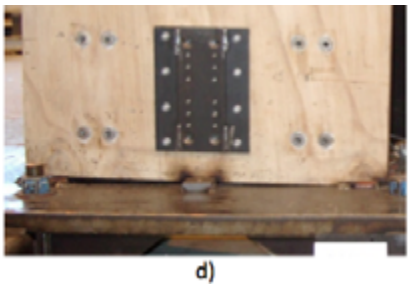

5 COMPARISON OF THE MBA AND WSA PROCEDURES

It is evident that there are significant differences between the MBA [9] and WSA design procedures. To illustrate this, a case study post-tensioned timber wall is considered.

The case study wall geometry and post-tensioning is based on existing real-world PT timber wall designs. For simplicity, additional reinforcement, such as u-shaped flexural plates, internal or external reinforcement is ignored. Note, the application of additional reinforcement simply introduces additional axial forces into the rocking connection, which should not affect the accuracy of the proposed approach.

Key design parameters are given in Table 2. Note, the PT tendons and timber are assumed to stay within the elastic range. Note, the appropriateness of these assumptions are investigated below.

Table 2: Design parameters for case study wall

Parameter	Symbol	Units	Value
Wall length	l_w	mm	3000
Wall thickness	t_w	mm	189
Shear span of wall	L_{cant}	mm	8310
Elastic modulus - timber	E_{para}	GPa	10.7
Gravity load	N_y	kN	40
No. of tendons	n_{PT}	-	2
Area of PT tendon	A_{PT}	mm^2	1608
Position of PT	x_{PT1}	mm	1350
Tendons to edge	x_{PT2}	mm	1650

Initial PT force	T_{Pti}	kN	696
Elastic modulus - PT	E_{PT}	GPa	170
Unbonded length of tendon	$l_{ub,PT}$	mm	13800

The connection moment, tendon forces, neutral axis depth and peak timber stresses are plotted versus the connection rotation in Figure 7. The connection moment and tendon forces predicted by the MBA approach are significantly less than that for the WBA approach. This is primarily because the timber strains and stresses according to the MBA approach are much smaller than the WMA (see Figure 7d). This is partly because the shear span for the case study structure is much larger than experimental specimens that were used to calibrate the MBA [9].

For similar reasons, the neutral axis depth predicted by the MBA approach is much larger than that for the WSA approach.

While under prediction of the connection moment may be acceptable to a designer (because the capacity is conservative), under-prediction of the peak stresses in the timber is a more serious concern. According the MBA approach, the timber does not yield up to 2% connection rotation. Yet, the WSA approach suggests that the timber will start yielding at less than 0.4% connection rotation. Commonly, PT walls target a connection rotation of approximately 1% for ULS actions. At this rotation significant timber crushing may have occurred. Furthermore, the initial assumption that the timber remains elastic is invalid for the WSA approach.

6 CONCLUSIONS

This paper provides an updated analytical design approach for assessing the connection response of rocking timber walls. This approach was calibrated using a finite element (FE) sensitivity study and validated using experimental data.

A strong correlation was achieved between the calibrated analytical relationship (for the neutral axis depth) and the results of 44 FE models. Furthermore, it was found that the deformation profile at the base of the walls was significantly non-linear, which has an impact of accuracy of the proposed design approaches.

It was demonstrated that an existing design approach, The Monolithic Beam Analogy, may significantly underestimate the peak stresses in the timber within the rocking connection.

Further experimental verification is recommended and should include different engineered wood products, wall geometries, axial stress levels and more precise evaluation of the neutral axis depth. Also, the appropriateness (or not) of the approach should be assessed when the compressive strength of the timber is exceeded.

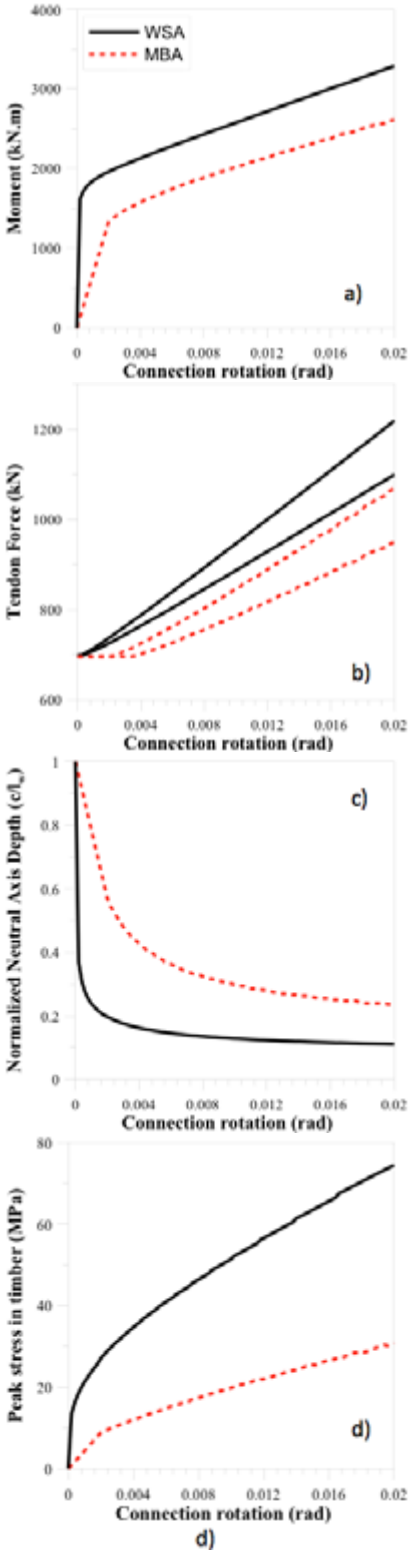

Figure 7: *WSA - MBA comparison for case study wall: a) Connection moment b) Tendon forces c) Neutral axis depth d) Peak timber stress*

7 ACKNOWLEDGEMENTS

Some of this research was performed during a doctorate [13] at the University of Canterbury, supervised by Prof. Stefano Pampanin and Prof. Andy Buchanan. Their support is gratefully acknowledged.

Input and review by Denis Pino and Dr Weng Yuen Kam is much appreciated.

8 REFERENCES

[1] Kolb, J., 2008, Systems in Timber Engineering, ed. Z. Lignum - Holzwirtschaft and M. DGfH - German Society of Wood Research. Berlin, Germany: Birkhauser.

[2] Palermo, A., et al., 2005, Seismic Design of Multi-Storey Buildings using Laminated Veneer Lumber (LVL). in 2005 New Zealand Society of Earthquake Engineering Conference. Wairaki, New Zealand.

[3] Kurama, Y.C., et al., 1999, Lateral load behavior and seismic design of unbonded post-tensioned precast concrete wall. PCI Journal, 46(4): pp. 622-633.

[4] Priestley, M.J.N., et al., 1999, Preliminary Results and Conclusions from the PRESSS Five-story Precast Concrete Test-Building. PCI Journal, 44(6): pp. 42-67.

[5] Rahman, A.M. and J.I. Restrepo, 2000, Earthquake Resistant Precast Concrete Buildings: Seismic Performance of Cantilever Walls Prestressed Using Unbonded Tendons, Department of Civil and Natural Resources Engineering, University of Canterbury: Christchurch, New Zealand.

[6] Pampanin, S., M.J.N. Priestley, and S. Sritharan, 2001, Analytical Modelling of the Seismic Behavior of Precast Concrete Frames Designed with Ductile Connections. Journal of Earthquake Engineering, 5(3): pp. 329-367.

[7] Palermo, A., 2004, Use of Controlled Rocking in the Seismic Design of Bridges, in Technical University of Milan, Technical Institute of Milan: Milan.

[8] NZS3101, 2006, Concrete Structures Standard: Appendix B: Special Provisions for Seismic Design of Ductile Jointed Precast Concrete Structural Systems. Vol. NZS3101:2006, Wellington: New Zealand Standards.

[9] Newcombe, M.P., et al., 2008, Section Analysis and Cyclic Behavior of Post-Tensioned Jointed Ductile Connections for Multi-Storey Timber Buildings. Journal of Earthquake Engineering, 12(Special Issue): pp. 83-110.

[10] Newcombe, M.P., 2008, Seismic Design of Multistorey Post-Tensioned Timber Buildings, in European School of Advanced Studies in Reduction of Seismic Risk (ROSE School), University of Pavia: Pavia, Italy. p. pp. 180.

[11] Marriott, D., 2009, The development of high-performance post-tensioned rocking systems for seismic design of structures, in Dept. of Civil and Nat. Res. Eng. , University of Canterbury: Christchurch, New Zealand. p. pp. 543.

[12] Pampanin, S., A. Palermo, and A.H. Buchanan, 2013, Post-Tensioned Timber Buildings, First Edition 2013, Part 2 Seismic design, University of Canterbury.

[13] Newcombe, M.P., 2012, Seismic Design of Post-Tensioned Timber Frame and Wall Buildings, in Department of Civil and Natural Resourses Engineering, University of Canterbury: Christchurch.

[14] SAP2000, 2005, Structural Analysis Package 2000, Version 10.0.1, Computers and Structures Inc.: Berkeley, California.

[15] Murray, Y.D., 2007, Manual for LS-DYNA wood material model 143, APTEK Inc.: Colorado Springs, U.S.A.

[16] Iqbal, A., et al., 2007, Application of Hysteretic Dampers in LVL Coupled Walls for Improved Seismic Performance. in Proceedings, 8th Pacific Conference of Earthquake Engineering, Singapore.

[17] Smith, T., et al., 2007, Seismic response of Hybrid-LVL coupled walls under quasi-static and pseudo-dynamic testing. in NZSEE Conference, Palmerston North, New Zealand.